Synthesis and Magnetostructural Characterization of Dinuclear Copper(II) Complexes with the Diazine Ligand, 3,6-Bis(di-2-pyridylmethyl)pyridazine *

Jorge Manzur,[a] Ana María García,[a] Ricardo Letelier,[a] Evgenia Spodine,[b] Octavio Peña,[c] Daniel Grandjean,[c] Marilyn M. Olmstead[d] and Bruce C. Noll[d]
[a] *Facultad de Ciencias Físicas y. Matemáticas, Universidad de Chile, Casilla 2777, Santiago, Chile*
[b] *Facultad de Ciencias Químicas y Farmacéuticas, Universidad de Chile, Casilla 233, Santiago, Chile*
[c] *U.A. au CNRS no. 254, Université de Rennes I, 35042 Rennes Cedex, France*
[d] *Department of Chemistry, University of California, Davis, CA 95616, USA*

The crystal structures of $[Cu_2(bdpdz)Br_4]\cdot 2CH_3CN$ **1**, $[Cu_2(bdpdz)Cl_3(H_2O)]Cl\cdot 3.5H_2O$ **2** and $[Cu_2(bdpdz)_2][ClO_4]_4$ **3** were determined by X-ray analysis, where bdpdz represents the binucleating ligand 3,6-bis(di-2-pyridylmethyl)pyridazine, formed by the reaction of 3,6-dichloropyridazine and di-2-pyridylmethyllithium. Compounds **1** and **2** consist of discrete binuclear units, in which copper atoms are linked by the diazine bridge and two halide ions. The pyridazine acts as a hexadentate ligand. In complex **2** the two copper(II) ions have a distorted octahedral co-ordination geometry, 4 + 2. Compound **3** also consists of discrete binuclear units, in which the copper centres are linked by two organic ligands. Here bdpdz acts as a pentadentate ligand, with one of the diazine nitrogen atoms not bonded. The two copper(II) ions have a square pyramidal co-ordination geometry, 4 + 1. The magnetic susceptibility was investigated in the temperature range 300–5 K. These measurements reveal an antiferromagnetic interaction for all three compounds ($-2J$ = 98.1 for **1**, 79.6 for **2** and 6.4 cm^{-1} for **3**). The lack of a diazine bridge, N–N, for the perchlorate salt **3** substantially reduces the antiferromagnetic interaction.

A variety of copper(II) complexes with binucleating ligands derived from pyridazine and phthalazine have been prepared. In these compounds multiple bridges between the copper atoms are formed with the presence of additional ligands such as hydroxide, halides or bidentate anions, leading to magnetic interactions between the metal centres. These compounds have been characterized from a magnetostructural point of view.[1–17]

Diazine ligands that generate six-membered chelate rings form complexes with copper–copper separations that fall in the range 3.00–3.14 Å, when Y is halide. When Y is NO_3^-, SO_4^{2-} or IO_3^- larger metal–metal separations result, 3.14–3.22 Å. Ligands that form five-membered chelate rings result in larger metal–metal separations (3.29–3.46 Å). Chloro-bridged complexes exhibit small exchange integrals ($-2J$ = 55–131 cm^{-1})[12,15,17] and much larger ones are obtained for the hydroxo-bridged compounds (190–1300 cm^{-1}).[3,6–8,10] In most cases an approximately distorted square-pyramidal geometry is observed for the copper centres, with a $d_{x^2-y^2}$ ground state.

In this report we describe the magnetostructural properties of $[Cu_2(bdpdz)Br_4]\cdot 2CH_3CN$ **1**, $[Cu_2(bdpdz)Cl_3(H_2O)]Cl\cdot 3.5H_2O$ **2** and $[Cu_2(bdpdz)_2][ClO_4]_4$ **3** [bdpdz = 3,6-bis(di-2-pyridylmethyl)pyridazine]. This previously unreported hexadentate ligand has two pyridine groups bonded in *ortho* positions on each side of the N–N fragment of the pyridazine molecule through a methyl group. This N_6 ligand bears a certain resemblance to the tetradentate ligands reported by Thompson and co-workers,[6–17] with the difference that it can produce octahedral instead of square-pyramidal species.

Table 1 Atomic coordinates (× 10^4) for $[Cu_2(bdpdz)Br_4]\cdot 2CH_3CN$ **1**

Atom	x	y	z
Cu	5673(1)	2684(1)	2129(1)
Br(1)	5489(1)	3720(1)	3461(1)
Br(2)	6221(1)	4950(1)	1771(1)
N(1)	5708(3)	1774(7)	989(4)
N(2)	6394(3)	1261(7)	2586(4)
N(3)	5229(2)	561(6)	2310(3)
C(1)	5595(3)	2671(10)	306(5)
C(2)	5624(4)	2096(10)	−475(5)
C(3)	5784(4)	517(12)	−565(5)
C(4)	5895(3)	−389(10)	119(5)
C(5)	5857(3)	271(8)	900(5)
C(6)	5960(3)	−734(8)	1676(4)
C(7)	6432(3)	−191(8)	2275(4)
C(8)	6872(3)	−1165(9)	2497(6)
C(9)	7284(3)	−623(10)	3048(6)
C(10)	7251(3)	886(11)	3363(5)
C(11)	6798(3)	1766(10)	3122(5)
C(12)	5450(3)	−791(8)	2113(4)
C(13)	5228(3)	−2252(8)	2296(4)
C(14)	8196(8)	1003(23)	522(13)
C(15)	7661(8)	295(29)	581(13)
C(16)	7405	4095	−644
C(17)	6886	4670	−321
C(18)	7354	5305	−435
C(19)	7123	4039	−630
N(4)	7277(12)	−155(36)	619(17)
N(5)	7780	4301	−773
N(6)	7765	5834	−530

Results

Structural Description of $[Cu_2(bdpdz)Br_4]\cdot 2CH_3CN$ **1**.— Table 1 lists the atomic parameters with estimated standard deviations. The copper complex lies along a crystallographic two-fold axis, so half of the structure is formed by rotation about this axis which lies in the plane formed by C(13), N(3), C(13a), N(3a). A drawing of the complex is shown in Fig. 1.

The structure consists of a binuclear copper(II) unit, with

---

* *Supplementary data available* (No. SUP 56923, 4 pp.): phase diagram. See Instructions for Authors, *J. Chem. Soc., Dalton Trans.*, 1993, Issue 1, pp. xxiii–xxviii.

Non SI unit employed: χ(cgs)/emu mol^{-1} = $(10^6/4\pi)\chi(SI)/m^3\ mol^{-1}$.

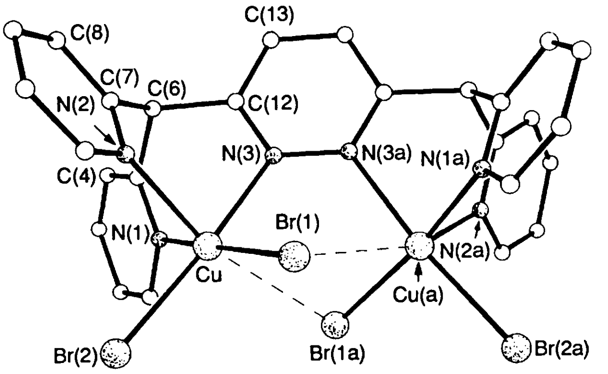

Fig. 1 A computer-generated drawing of $[Cu_2(bdpdz)Br_4]$ **1**

Table 2 Selected bond lengths (Å) and angles (°) for $[Cu_2(bdpdz)Br_4]\cdot 2CH_3CN$ **1**

Cu–Br(1)	2.421(1)	Cu–N(1)	2.016(6)
Cu–Br(2)	2.460(1)	Cu–N(3)	2.147(6)
Cu–Br(1a)	3.080(1)	Cu–N(2)	2.223(6)
Cu ··· Cu(a)	3.673(2)	N(3)–N(3a)	1.351(12)
N(1)–Cu–Br(2)	90.3(2)	N(2)–Cu–Br(2)	93.2(2)
N(1)–Cu–N(3)	82.8(2)	N(2)–Cu–Br(1)	96.8(2)
Br(2)–Cu–Br(1)	95.0(1)	N(2)–Cu–N(3)	84.7(2)
Br(1)–Cu–N(3)	92.0(2)	Br(1a)–Cu–N(1)	87.1(2)
N(1)–Cu–Br(1)	171.5(2)	Br(1a)–Cu–Br(2)	103.2(1)
Br(2)–Cu–N(3)	172.8(2)	Br(1a)–Cu–Br(1)	85.2(1)
Cu–Br(1)–Cu(a)	82.9(1)	Br(1a)–Cu–N(3)	78.6(2)
Cu–N(3)–N(3a)	122.2(2)	Br(1a)–Cu–N(2)	163.3(2)
N(2)–Cu–N(1)	89.4(2)		

the organic ligand bridging the two metal centres through the pyridazine moiety. There are two bromide bridges [Cu–Br(1a) = Cu(a)–Br(1) 3.080(1) Å]. The two copper–bromide–copper bridging angles are Cu–Br(1a)–Cu(a) = Cu(a)–Br(1)–Cu 82.9(1)°. The geometry at each copper(II) centre is a significantly distorted octahedron, 4 + 2. The basal plane for the copper atom is described by the pyridazine nitrogen atom N(3), one pyridine nitrogen atom N(1), one terminal bromide atom Br(2), and one bridging bromine atom Br(1). The axial sites are occupied by the bromine atom Br(1a), which is basal to the other copper in the dimer, and by the nitrogen atom of the second pyridine ring N(2) of the di-2-pyridylmethyl substituent. The basal Cu–Br distances are Cu–Br(1) = Cu(a)–Br(1a) 2.421(1) and Cu–Br(2) = Cu(a)–Br(2a) 2.460(1) Å. The basal copper–nitrogen distances are Cu–N(1) 2.016(6) and Cu–N(3) 2.147(6) Å, while the apical distance is Cu–N(2) 2.223(6) Å. The Cu ··· Cu(a) distance is 3.673(2) Å. The bond distances and angles about the copper(II) atoms are given in Table 2.

Ionic bromide is not observed in complex **1**, while the solvent molecules are all disordered, filling voids in the crystal structure. The acetonitrile C(14)–C(15)–N(4) was modelled at 50% occupancy to produce a single molecule per formula unit; C(17)–C(16)–N(5) and C(19)–C(18)–N(6) each occupy their sites 25% of the time to yield another full molecule between them.

The bromo-bridged complex undergoes a phase transition (SUP 56923) with change of temperature, which is completely reversible. This phenomenon was monitored by the intensity of six measured reflections through thirteen observations at eleven temperatures from −57 to −138 °C. The transition seems to occur at approximately −114 °C. However, it is not clear where the end of the transition range is. The material continued to change until the lower limit of the low-temperature device was reached.

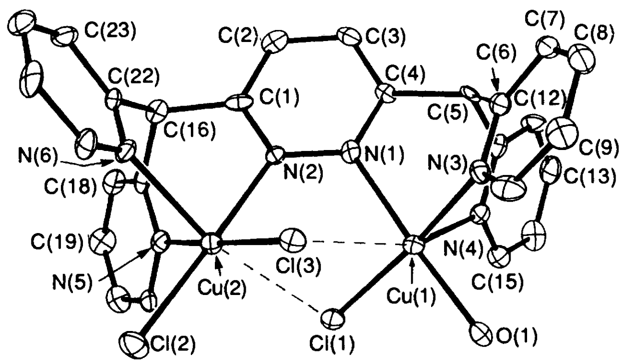

Fig. 2 A computer-generated drawing of $[Cu_2(bdpdz)Cl_3(H_2O)]Cl$ **2**

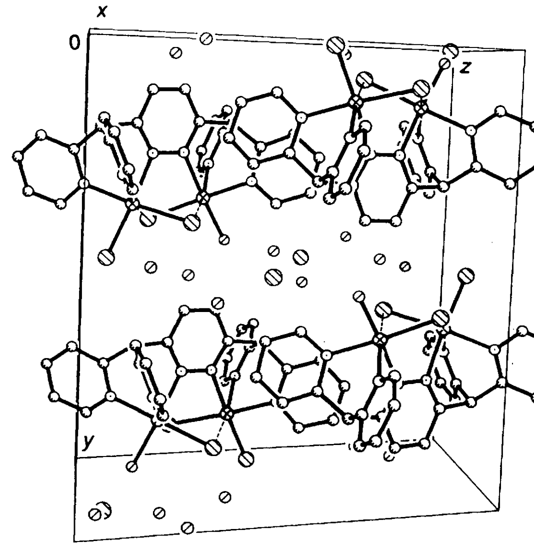

Fig. 3 A perspective view of complex **2** showing the water molecules in the structure as viewed down the crystallographic *a* axis. ⊘, Oxygen atoms of water molecules

Structural Description of $[Cu_2(bdpdz)Cl_3(H_2O)]Cl\cdot 3.5H_2O$ **2**.—Table 3 lists the atomic parameters with estimated standard deviations. The structure consists of a binuclear copper(II) asymmetric unit, with the organic ligand bridging the two metal centres through the pyridazine moiety. As depicted in Fig. 2, there are two halide bridges represented by the long copper–halogen bonds Cu(1)–Cl(3) 2.931(2) and Cu(2)–Cl(1) 2.873(2) Å. The two copper–chloride–copper bridging angles are Cu(1)–Cl(1)–Cu(2) 85.3(1) and Cu(2)–Cl(3)–Cu(1) 83.4(1)°. The Cu(1) ··· Cu(2) distance within the molecule is 3.511(1) Å, while the closest intermolecular Cu ··· Cu distance is 7.656 Å. The ionic Cl(4) is 3.069 Å from the co-ordinated water O(1). In addition to the co-ordinated water there are 3.5 additional water molecules which tend to form a channel in the structure. The crystal packing of complex **2** and of the water molecules is shown in Fig. 3.

The geometry at each copper(II) centre is a significantly distorted octahedron. Alternatively the distortion may be thought of as arising from a 4 + 2 semico-ordinate geometry. The basal plane for Cu(1) is made up of one pyridazine nitrogen atom N(1), one pyridine nitrogen atom N(3), one chloride ion Cl(1) and one oxygen atom from a water molecule. The axial sites are occupied by the chloride ion Cl(3), which is basal to the other copper in the dimer and by the nitrogen atom of the second pyridine ring N(4) of the 2-pyridylmethyl substituent. The basal plane for Cu(2) is different, and is made up of one pyridazine nitrogen atom N(2), one pyridine nitrogen atom N(5), and two chloride atoms, Cl(2) (terminal) and Cl(3) (bridging). The apical positions are occupied by the bridging chloride ion Cl(1) and by the nitrogen atom of the second

Table 3 Atomic coordinates (× 10^4) for $[Cu_2(bdpdz)Cl_3(H_2O)]Cl{\cdot}3.5H_2O$ **2**

Atom	*x*	*y*	*z*
Cu(1)	3 391(1)	8 658(1)	1 990(1)
Cu(2)	2 330(1)	8 744(1)	3 801(1)
Cl(1)	4 320(1)	9 214(1)	3 342(1)
Cl(2)	1 937(2)	9 925(1)	4 400(1)
Cl(3)	1 277(1)	9 098(1)	2 357(1)
O(1)	3 667(4)	9 654(3)	1 376(3)
O(2)	7 489(4)	9 774(4)	3 460(3)
O(3)	5 670(4)	10 374(3)	2 009(3)
O(4)	9 045(5)	10 085(4)	2 514(3)
O(5)	9 398(13)	9 594(9)	437(9)
N(1)	3 001(4)	7 610(3)	2 548(3)
N(2)	2 778(4)	7 633(3)	3 326(3)
N(3)	2 343(4)	8 214(3)	824(3)
N(4)	4 828(5)	7 935(3)	1 799(3)
N(5)	3 382(4)	8 359(3)	4 994(3)
N(6)	940(4)	8 034(3)	4 082(3)
C(1)	2 676(5)	6 960(3)	3 738(4)
C(2)	2 763(5)	6 203(4)	3 374(4)
C(3)	2 952(5)	6 177(4)	2 565(4)
C(4)	3 079(5)	6 902(3)	2 176(4)
C(5)	3 338(5)	6 933(3)	1 298(4)
C(6)	2 427(5)	7 426(4)	621(4)
C(7)	1 698(6)	7 102(4)	−166(4)
C(8)	891(6)	7 586(4)	−768(4)
C(9)	816(6)	8 383(4)	−569(4)
C(10)	1 549(5)	8 672(4)	236(4)
C(11)	4 570(5)	7 195(4)	1 458(4)
C(12)	5 383(6)	6 675(4)	1 321(4)
C(13)	6 512(6)	6 944(4)	1 539(4)
C(14)	6 796(6)	7 702(4)	1 886(4)
C(15)	5 925(6)	8 180(4)	2 000(4)
C(16)	2 447(5)	7 040(4)	4 621(4)
C(17)	3 333(5)	7 592(4)	5 256(4)
C(18)	4 083(6)	7 321(4)	6 061(4)
C(19)	4 872(6)	7 841(4)	6 624(4)
C(20)	4 898(6)	8 620(4)	6 358(4)
C(21)	4 167(5)	8 867(4)	5 543(4)
C(22)	1 192(5)	7 302(3)	4 428(4)
C(23)	369(6)	6 802(4)	4 572(4)
C(24)	−753(6)	7 067(4)	4 356(4)
C(25)	−1 020(6)	7 836(4)	4 003(4)
C(26)	−153(6)	8 295(4)	3 877(4)
Cl(4)	2 045(2)	5 027(1)	5 633(1)

Table 4 Selected bond lengths (Å) and angles (°) for $[Cu_2(bdpdz)Cl_3(H_2O)]Cl{\cdot}3.5H_2O$ **2**

Cu(1)–Cl(1)	2.266(2)	Cu(2)–Cl(2)	2.298(2)
Cu(1)–N(1)	2.078(5)	Cu(2)–N(2)	2.133(5)
Cu(1)–N(3)	2.013(4)	Cu(2)–N(6)	2.236(6)
Cu(1)–O(1)	2.005(4)	Cu(2)–Cl(1)	2.873(2)
Cu(1)–N(4)	2.236(6)	Cu(2)–N(5)	2.013(5)
Cu(1)–Cl(3)	2.931(2)	Cu(2)–Cl(3)	2.302(2)
Cu(1) ··· Cu(2)	3.511(1)	N(1)–N(2)	1.345(8)
N(3)–Cu(1)–N(1)	85.1(2)	N(6)–Cu(2)–Cl(2)	95.3(1)
N(3)–Cu(1)–O(1)	91.1(2)	N(6)–Cu(2)–N(2)	85.0(2)
O(1)–Cu(1)–Cl(1)	90.3(1)	N(2)–Cu(2)–Cl(1)	79.0(1)
Cl(1)–Cu(1)–N(1)	93.3(1)	Cl(1)–Cu(2)–Cl(2)	100.4(1)
O(1)–Cu(1)–N(1)	175.9(2)	Cl(1)–Cu(2)–N(6)	163.9(1)
N(3)–Cu(1)–Cl(1)	171.2(2)	Cl(2)–Cu(2)–N(2)	176.3(1)
N(4)–Cu(1)–O(1)	96.5(2)	N(5)–Cu(2)–Cl(1)	89.1(1)
N(4)–Cu(1)–Cl(1)	99.8(1)	N(5)–Cu(2)–N(2)	83.9(2)
N(4)–Cu(1)–N(1)	84.7(2)	N(5)–Cu(2)–N(6)	86.7(2)
N(4)–Cu(1)–N(3)	88.6(2)	N(5)–Cu(2)–Cl(2)	92.4(2)
Cl(3)–Cu(1)–O(1)	100.9(1)	Cl(3)–Cu(2)–Cl(1)	86.0(1)
Cl(3)–Cu(1)–Cl(1)	85.3(1)	Cl(3)–Cu(2)–N(2)	90.0(1)
Cl(3)–Cu(1)–N(1)	77.6(1)	Cl(3)–Cu(2)–N(6)	96.5(1)
Cl(3)–Cu(1)–N(3)	86.0(1)	Cl(3)–Cu(2)–Cl(2)	93.7(1)
Cl(3)–Cu(1)–N(4)	161.8(1)	Cl(3)–Cu(2)–N(5)	172.8(2)
Cu(1)–Cl(1)–Cu(2)	85.3(1)	Cu(1)–N(1)–N(2)	120.5(4)
Cu(1)–Cl(3)–Cu(2)	83.4(1)	Cu(2)–N(1)–N(2)	119.9(4)

pyridine ring N(6) of the other 2-pyridylmethyl substituent at *para* position in relation to a similar one in the pyridazine ring. The basal Cu–Cl distances are Cu(1)–Cl(1) 2.266(2), Cu(2)–Cl(2) 2.298(2), Cu(2)–Cl(3) 2.302(2) Å, while the basal Cu–N distances are Cu(1)–N(1) 2.078(5), Cu(1)–N(3) 2.013(4), Cu(2)–N(2) 2.133(5), Cu(2)–N(5) 2.013(5), Cu(1)–O(1) 2.005(4) Å. The two longer apical distances are Cu(1)–N(4) 2.236(6) and Cu(2)–N(6) 2.236(6) Å. The bond distances and angles about the copper(II) ions are given in Table 4.

Structural Description of $[Cu_2(bdpdz)_2][ClO_4]_4$ **3**.—Table 5 lists the atomic parameters with estimated standard deviations. The structure of compound **3** consists of a binuclear copper(II) unit linked by two bdpdz ligands (Fig. 4). In this case the organic molecule is bonded through five of its nitrogen atoms, giving five-co-ordinate metal centres. One of the diazine nitrogen atoms remains unco-ordinated, thus presenting a different co-ordination behaviour compared to compounds **1** and **2**. The N–N distance in the diazine unit is N(7)–N(8) 1.361(7) and N(1)–N(2) 1.345(7) Å. These values are closely related to the distances observed in the chloro- and bromo-bridged complexes, where the organic molecule acts as an hexadentate ligand.

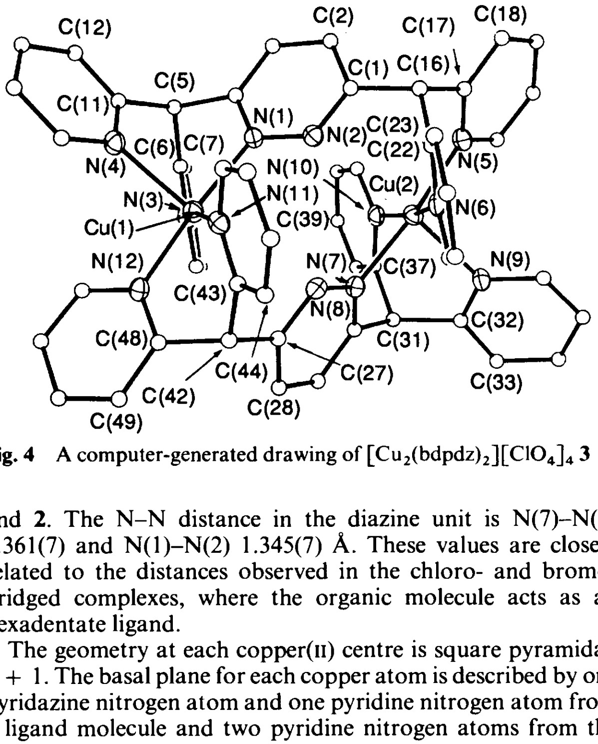

Fig. 4 A computer-generated drawing of $[Cu_2(bdpdz)_2][ClO_4]_4$ **3**

The geometry at each copper(II) centre is square pyramidal, 4 + 1. The basal plane for each copper atom is described by one pyridazine nitrogen atom and one pyridine nitrogen atom from a ligand molecule and two pyridine nitrogen atoms from the second ligand [Cu(1)–N(1) 2.049(5), Cu(1)–N(3) 2.024(5), Cu(1)–N(11) 2.003(5), Cu(1)–N(12) 2.001(5); Cu(2)–N(7) 2.038(5), Cu(2)–N(10) 2.039(5), Cu(2)–N(5) 2.014(5), Cu(2)–N(6) 2.000(5) Å]. The apical position corresponds to a pyridine nitrogen atom of the first ligand related to each copper centre [Cu(1)–N(4) 2.175(5), Cu(2)–N(9) 2.176(5) Å]. Selected bond distances and angles are given in Table 6.

The dimeric compound is a perchlorate salt with one of the perchlorates disordered. This was refined with two sets of oxygen atoms at relative weights of $\frac{2}{3}:\frac{1}{3}$. There is no interaction between the perchlorates and the metal centres. The copper atoms are at a distance of 4.809(2) Å.

Magnetic Susceptibility.—The susceptibility is plotted as a function of temperature in Fig. 5. The dominant features of the data are maxima near 90 for complex **1**, 70 for **2**, and 6 K for **3** indicating antiferromagnetic coupling within the dimers, and a

Table 5 Atomic coordinates (× 10^4) for $[Cu_2(bdpdz)_2][ClO_4]_4$ **3**

Atom	*x*	*y*	*z*	Atom	*x*	*y*	*z*
Cu(1)	4364(1)	7853(1)	1077(1)	N(1)	3423(4)	6367(4)	1173(1)
Cu(2)	732(1)	7692(1)	1514(1)	N(2)	2881(4)	6314(4)	1466(1)
Cl(1)	377(1)	8050(2)	4366(1)	N(3)	3561(4)	7909(5)	633(1)
Cl(2)	3431(1)	2426(2)	152(1)	N(4)	5538(4)	6615(5)	859(1)
Cl(3)	2041(2)	1875(2)	2262(1)	N(5)	−49(4)	6134(4)	1610(1)
Cl(4)	5108(2)	3773(2)	1768(1)	N(6)	1460(4)	7539(4)	1962(1)
O(1)	1337(4)	7636(6)	4211(2)	N(7)	1617(4)	9172(4)	1382(1)
O(2)	−158(5)	7002(5)	4500(1)	N(8)	2680(4)	9224(4)	1473(1)
O(3)	−293(5)	8611(5)	4128(2)	N(9)	−595(4)	8919(5)	1628(1)
O(4)	649(4)	8867(4)	4633(1)	N(10)	272(4)	7684(4)	1022(1)
O(5)	2858(4)	3552(4)	150(1)	N(11)	4850(4)	8078(4)	1553(1)
O(6)	3476(4)	1978(5)	490(1)	N(12)	5122(4)	9398(5)	965(1)
O(7)	4510(4)	2587(5)	29(1)	C(1)	2269(5)	5354(6)	1522(2)
O(8)	2872(4)	1584(4)	−58(1)	C(2)	2184(5)	4389(6)	1298(2)
O(9)	2150(4)	3122(4)	2349(1)	C(3)	2725(5)	4473(5)	1002(2)
O(10)	1417(5)	1293(5)	2516(2)	C(4)	3334(5)	5498(5)	945(2)
O(11)	1498(5)	1772(6)	1949(2)	C(5)	3908(5)	5732(6)	613(2)
O(12)	3076(4)	1312(4)	2239(1)	C(6)	3418(5)	6865(6)	465(2)
O(13)	5386(7)	2576(7)	1865(2)	C(7)	2758(5)	6819(6)	186(2)
O(14)	5519(8)	4320(8)	1466(2)	C(8)	2262(6)	7851(6)	76(2)
O(15)	4814(9)	4514(9)	2016(3)	C(9)	2419(5)	8926(6)	244(2)
O(16)	4054(8)	3219(1)	1642(2)	C(10)	3084(5)	8919(6)	517(2)
O(13A)	5892(12)	2846(13)	1804(3)	C(11)	5126(5)	5743(6)	661(2)
O(14A)	5068(15)	4166(16)	1436(5)	C(12)	5762(5)	4858(6)	522(2)
O(15A)	4163(11)	4267(11)	1942(3)	C(13)	6872(6)	4866(6)	588(2)
O(16A)	6022(9)	4450(10)	1976(3)	C(14)	7294(6)	5736(6)	785(2)

Table 6 Selected bond lengths (Å) and angles (°) for $[Cu_2(bdpdz)_2]$-$[ClO_4]_4$ **3**

Cu(1)–N(1)	2.049(5)	Cu(2)–N(7)	2.038(5)
Cu(1)–N(11)	2.003(5)	Cu(2)–N(5)	2.014(5)
Cu(1)–N(12)	2.001(5)	Cu(2)–N(6)	2.000(5)
Cu(1)–N(3)	2.024(5)	Cu(2)–N(10)	2.039(5)
Cu(1)–N(4)	2.175(5)	Cu(2)–N(9)	2.176(5)
N(1)–N(2)	1.345(7)	N(7)–N(8)	1.361(7)
Cu(1) ··· Cu(2)	4.809(2)		
N(4)–Cu(1)–N(12)	98.0(2)	N(6)–Cu(2)–N(9)	101.8(2)
N(4)–Cu(1)–N(1)	86.8(2)	N(5)–Cu(2)–N(9)	97.8(2)
N(3)–Cu(1)–N(4)	89.8(2)	N(7)–Cu(2)–N(9)	87.4(2)
N(4)–Cu(1)–N(11)	104.9(2)	N(9)–Cu(2)–N(10)	89.7(2)
N(1)–Cu(1)–N(3)	84.9(2)	N(5)–Cu(2)–N(6)	88.4(2)
N(1)–Cu(1)–N(11)	95.3(2)	N(6)–Cu(2)–N(7)	93.3(2)
N(3)–Cu(1)–N(12)	90.4(2)	N(5)–Cu(2)–N(10)	92.6(2)
N(11)–Cu(1)–N(12)	88.0(2)	N(7)–Cu(2)–N(10)	84.5(2)
N(3)–Cu(1)–N(11)	165.3(2)	N(5)–Cu(2)–N(7)	174.1(2)
N(1)–Cu(1)–N(12)	173.3(2)	N(6)–Cu(2)–N(10)	168.2(2)
Cu(1)–N(1)–N(2)	118.6(4)	Cu(2)–N(7)–N(8)	118.8(4)

rapid increase at low temperature, corresponding to monomeric impurities with paramagnetic behaviour.

The model of an isolated Heisenberg dimer of $S = \frac{1}{2}$ ions with Hamiltonian interaction $H = -2JS_1 \cdot S_2$ has been used to analyse the data. The susceptibility of this model is described by the Bleaney–Bowers equation.[18] The best fit was calculated from the modified equation (1) for exchange-coupled pairs of

$$\chi_M = N\beta^2 g^2/3kT[1 + \tfrac{1}{3}\exp(-2J/kT)]^{-1}(1 - p) + (N\beta^2 g^2/4kT)p + N\alpha \quad (1)$$

copper(II) ions, where in this expression $2J$ is the singlet–triplet splitting, p represents the fraction of a possible magnetically dilute copper(II) impurity, and $N\alpha$ the temperature-independent paramagnetism for a binuclear copper(II) complex taken as 120×10^{-8} emu mol^{-1}. The results of the fit are shown in Fig. 5 and the best-fit parameters are $J = -49.5$ cm^{-1}, $g = 2.08$ and $p = 0.024$ for **1**, -39.8 cm^{-1}, 2.20 and 0.026 for **2** and -3.2 cm^{-1}, 2.05 and 0.002 for **3**. The experimental magnetic data for complex **1** are well fitted with the Bleaney–Bowers equation, even though a phase transition is observed near the maximum in the magnetic susceptibility curve. The exact structure of the dimeric complex is not known at low temperatures, but evidently does not influence the magnetic interaction which is between the two metal centres.

Discussion

Binucleating tetradentate pyridazine and phthalazine ligands in general form binuclear copper(II) complexes involving a hydroxide bridge in addition to the diazine bridge. Two such ligands, 3,6-di(2-pyridylthio)pyridazine (dppdz) and 1,4-bis-(4,6-dimethyl-2-pyridylamino)phthalazine (bdplz) have been shown to form not only hydroxo-bridged derivatives, but also dihalogeno bridged compounds $[Cu_2(dppdz)X_4]$ (X = Cl or Br) and $[Cu_2(bdplz)Cl_4]$.[12,15,17] Structural parameters and magnetic data for these complexes and for the studied compounds are given in Table 7.

A comparison of the structural parameters of $[Cu_2(dppdz)Cl_4]\cdot CH_3CH_2OH$ **4** with those obtained for compound **2** reveals that the copper–copper distance is shorter for **4** (3.198 Å) than for **2** [3.51(Å)]. This can be attributed in part to the presence of an extra pyridine ring in **2**, in relation to **4**, a feature which increases the co-ordination sphere of the metal centres from five to six. The chlorine bridge angles, which are 79.65 and 81.70° for **4**, also increase for **2** to 83.4 and 85.3°. Each chlorine bridge forms an axial and an equatorial interaction with the copper centres in **4**, leading to one long copper–chlorine bond (2.60–2.70 Å) and one short bond (2.27 Å). A similar situation is observed in **2**, leading to one long copper–chlorine bond (2.93–2.87 Å) and one short bond (2.27–2.30 Å).

The asymmetric nature of the chlorine bridging network in both **2** and **4** leads to an interesting situation with respect to the magnetic properties of these systems. This makes magnetic exchange *via* the chloride bridges less probable because only one copper orbital per chloride bridge is a magnetic orbital. This is based on the assumption that the copper ion ground state is $d_{x^2-y^2}$ and only one magnetic orbital lobe per copper is directed towards a chloride bridge. The other bridging interaction to each copper centre involves an axial orbital. This effectively orthogonal situation would,

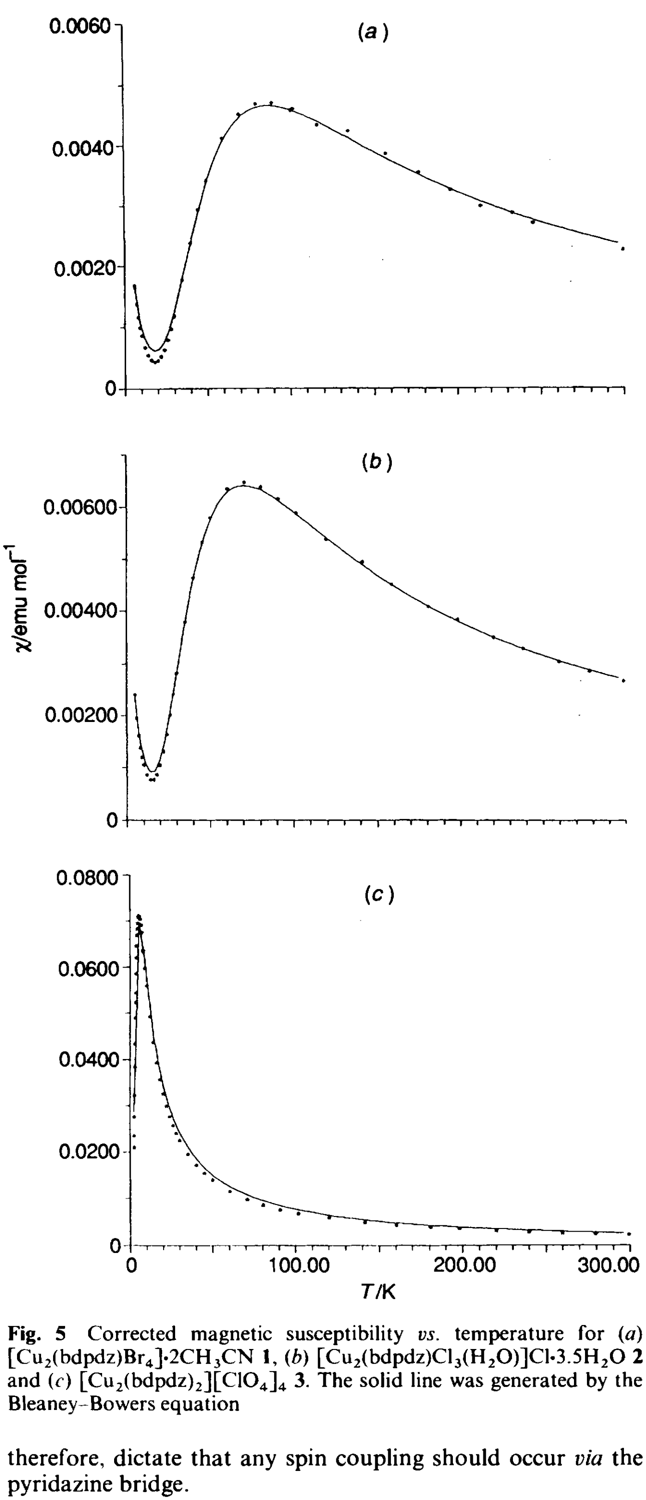

Fig. 5 Corrected magnetic susceptibility *vs.* temperature for (*a*) $[Cu_2(bdpdz)Br_4]\cdot 2CH_3CN$ **1**, (*b*) $[Cu_2(bdpdz)Cl_3(H_2O)]Cl\cdot 3.5H_2O$ **2** and (*c*) $[Cu_2(bdpdz)_2][ClO_4]_4$ **3**. The solid line was generated by the Bleaney–Bowers equation

therefore, dictate that any spin coupling should occur *via* the pyridazine bridge.

A comparison of the magnetic data for **2** and **4** indicates greatly enhanced exchange in the case of complex **4** with the tetradentate ligand, in relation to **2** with the hexadentate ligand. The increased copper–copper separation in **2** is accompanied by an increase in the diazine N–N separation [1.345(8) Å for **2**, 1.316(9) Å for **4**]. The copper–nitrogen (diazine) distances are also larger in compound **2** as compared to **4**; so are the Cu–N–N (diazine) angles (**2**, 120.5 and 119.9; **4**, 118.0 and 116.0°). All these structural differences might be expected to weaken the exchange *via* the pyridazine molecule, if this bridge is to be considered as the superexchange pathway responsible for the antiferromagnetic coupling.

The idea that the diazine bridge is the pathway for the magnetic coupling can be considered as probable if one takes into account that the monochloro-bridged complex $[Cu_2(dppdz)_2Cl][ClO_4]_3$ **5** in which the two square-pyramidal copper(II) atoms are bridged axially by the chloride and equatorially by the organic molecules in a symmetrical way, exhibits strong antiferromagnetism ($-2J$ = 480 cm^{-1}). The axial position of the chloride creates an orthogonal situation where no coupling should take place, and the two pyridazine molecules which bridge the metal centres *via* the magnetic $d_{x^2-y^2}$ orbital should be responsible for the exchange phenomenon that is observed.[17] This argument is reinforced if the value of $2J = -6.4$ cm^{-1} for $[Cu_2(bdpdz)_2][ClO_4]_4$ **3** is taken into account. In this complex the N–N bridge is lost since the organic ligand bbpdz links only through one of the diazine nitrogen atoms to one metal centre.

Since the exchange of the pyridazine-derived complex **4** is substantially larger than that observed for the mentioned phthalazine-derived complex **6**, it is reasonable to assume that the pyridazine bridge is a better superexchange medium than phthalazine ($2J = -131$ for **4** and -55 cm^{-1} for **6**). As was already stated, both complexes are dibridged chloro complexes in which the chloride bridge has an equatorial and axial interaction with each of the copper centres, therefore not serving as a pathway for magnetic interaction. These data also reinforce the idea that the superexchange is *via* the diazine bridge.

On the assumption that the diazine bridge of a particular organic molecule provides a roughly constant contribution to the total exchange, the variations of the observed phenomena could be partly attributed to the peripheral donors. If these are bound axially they should not influence the copper magnetic orbitals from an electronic point of view. Therefore, the extra pyridine ring found in the bdpdz complexes **1** and **2** should not participate in the magnetic phenomenon. If the ligands are bound in the equatorial planes of the copper centres they can be considered to have a significant influence on the metal magnetic orbital.

The effect of non-bridging equatorial ligands should be seen in the bromo analogues of **2** and **4**. The less-electronegative bromine atom would, therefore, be expected to polarize the electron density in this bond, and hence in the copper magnetic orbital to a lesser extent than chlorine, thus effectively allowing more electron density in the copper magnetic orbital to participate in the exchange process with greater resulting exchange. The effect of replacing chlorine by bromine on the exchange is effectively illustrated by comparing **4** ($2J = -131$ cm^{-1}) with the isostructural complex $[Cu_2(dppdz)Br_4]$ **7**, which has a much larger exchange ($2J = -243$ cm^{-1}). For the bromo complex **1** the antiferromagnetic exchange increases, from $2J = -79.6$ cm^{-1} for the chloro to -98.1 cm^{-1}. This enhancement is significantly lower than observed for the dppdz complexes. The exact reason for the difference is not well understood. A complex of similar stoichiometry to **2** is $[Cu_2(bppdz)Cl_4(H_2O)]$ **8** [bppdz = 3,6-bis(2-pyridyl)pyridazine].[1] Even though the organic ligand is tetradentate, it corresponds to the binucleating ligands which generate five-membered chelate rings with each metal centre. In **8** the square-pyramidal co-ordination is achieved by one bridging chlorine, two nitrogen and two terminal chlorine atoms for Cu(2), and one terminal chlorine atom and a water molecule for Cu(1). The copper–copper separation is 3.51 Å, comparable to the value found for **2**, even though **8** has five-membered chelate rings at each metal centre and **2** has six-membered chelate rings.

In general the effect of changing the chelate ring size from six to five has been shown to increase copper–copper separations. However, in the present case this effect is not observed. The magnetic properties cannot be compared because no data have been reported for compound **8**. It can be concluded that the novel bdpdz ligand is not a very efficient bridge for the transmission of the magnetic interaction through the N–N diazine bridge, when it acts as a hexadentate ligand generating octahedral species. The efficiency is even lower when the ligand is pentadentate and does not bond through both N–N atoms.

Table 7 Magnetic and structural data

Compound	Ref.	$-2J$/cm^{-1}	g	Cu · · · Cu/Å	Cu–N/Å (diazine)	N–N/Å (diazine)	Cu–X/Å (bridge)
1 $[Cu_2(bdpdz)Br_4]\cdot 2CH_3CN$	This work	98.1	2.08	3.673(2)	2.147(6)	1.351(12)	3.080(1) 2.421(1)
2 $[Cu_2(bdpdz)Cl_3(H_2O)]Cl\cdot 3.5H_2O$	This work	79.6	2.20	3.511(1)	2.078(5)	1.345(8)	2.302(2) 2.873(2) 2.266(2) 2.931(2)
3 $[Cu_2(bdpdz)_2][ClO_4]_4$	This work	6.4	2.05	4.809(2)	2.049(5) 2.038(5)	1.345(7) 1.361(7)	No bridge
4 $[Cu_2(dppdz)Cl_4]\cdot CH_3CH_2OH$	12	130.5	2.029	3.198(1)	2.075(6) 2.069(5)	1.316(9)	2.269(2) 2.698(2) 2.268(2) 2.605(2)
5 $[Cu_2(dppdz)_2Cl][ClO_4]_3\cdot CH_3CN$	17	479	2.190	3.269(2)	2.018(5) 2.018(5) 1.994(6) 1.994(6)	—	2.448(3) 2.430(3)
6 $[Cu_2(bdplz)Cl_4]$	12	55.2	2.052	3.251(1)	2.022(2)	1.385(5)	2.277(1) 2.589(1)
7 $[Cu_2(dppdz)Br_4]$	15	243.5	2.072	3.318(3)	2.081(12) 2.070(13)	1.366(19)	2.414(3) 2.801(3) 2.380(3) 2.766(3)
8 $[Cu_2(bppdz)Cl_4(H_2O)]$	1	—	—	3.51	2.027(9) 2.039(10)	1.286(12)	2.130(6) 2.168(6)

Experimental

Syntheses.—3,6-*Bis*(*di*-2-*pyridylmethyl*)*pyridazine*. A solution of 3,6-dichloropyridazine in diethyl ether was added to di-2-pyridylmethyllithium [obtained from the reaction of di-2-pyridylmethane[19] and butyllithium (Aldrich)] in a 1:2 molar ratio, dissolved in the same solvent (100 cm^3) at −15 °C. The reaction mixture was left to stand until room temperature was reached. The excess of butyllithium was then eliminated with water and the mixture stirred for 1 h. The solid product was filtered off and recrystallized from an ethanol–ether solution. The ligand was identified by IR and ^{1}H NMR spectroscopy.

$[Cu_2(bdpdz)Br_4]\cdot 2CH_3CN$ **1** *and* $[Cu_2(bdpdz)Cl_3(H_2O)]Cl\cdot 3.5H_2O$ **2**. A solution of bdpdz (1 mmol) in methanol (15 cm^3) was added to a warm solution (5 cm^3) of $CuBr_2$ or $CuCl_2\cdot 2H_2O$ (3 mmol) in the same solvent. The precipitate obtained was recrystallized from a water–CH_3CN solution (yield: 80 **1**, 75% **2**).

$[Cu_2(bdpdz)_2][ClO_4]_4$ **3**. A solution of bdpdz (1 mmol) in methanol (15 cm^3) was added to a solution of $Cu(ClO_4)_2\cdot 6H_2O$ (2 mmol) in acetonitrile (5 cm^3). On standing blue crystals suitable for X-ray diffraction separated (yield: 70%).

X-Ray Crystallography.—Crystals of the compounds **1**–**3** were removed from their mother-liquor and immediately coated with a protective coating of a hydrocarbon oil. The crystals selected for data collection were mounted in the cold stream of the diffractometer and exhibited no decay in the intensities of standard reflections thereafter. Crystallographic programs employed were the Siemens data collection software and SHELXTL PLUS.[20] Scattering factors were from ref. 21.

Crystal data for complex **1**. $C_{30}H_{26}Br_4Cu_2N_8$, M = 945.3, monoclinic, space group $C2/c$, a = 24.866(6), b = 8.478(2), c = 16.237(4) Å^3 (by least-squares refinement on diffractometer angles for 24 centred reflections, T = 216 K), Z = 4, D_c = 1.84 g cm^{-3}, $F(000)$ = 1792, orange plates, crystal dimensions 0.05 × 0.22 × 0.25 mm, μ(Mo-Kα) = 5.96 mm^{-1}.

Data collection and processing. Syntex P2$_1$ diffractometer, T = 216 K, ω scans with ω scan width 1.0°, ω scan speed 6° min^{-1}, graphite-monochromated Mo-Kα radiation, 2θ range 0–55°, $+h$, $+k$, $\pm l$; 4573 reflections measured, 3920 unique [R(merge) = 0.026], 2746 with $I > 2\sigma(I)$. Empirical absorption correction, XABS,[22] transmission factors 0.34–0.78.

Structure analysis and refinement. Patterson (Cu and Br) and Fourier difference methods. Full-matrix least-squares refinement with all except acetonitriles and non-hydrogen atoms anisotropic and hydrogens riding on bonded carbons, U_{iso} fixed at 0.04 or 0.05 Å^2; $w = [\sigma^2(F) + 0.0063F^2]^{-1}$. Refinement converged to R = 0.0572 and R' = 0.0590.

Crystal data for complex **2**. $C_{26}H_{29}Cl_4Cu_2N_6O_{4.5}$, M = 766.4, monoclinic, space group $P2_1/c$, a = 12.278(4), b = 16.635(4), c = 15.803(4) Å, β = 109.01(2)°, U = 3031(1) Å^3 (by least-squares refinement on diffractometer angles for 28 centred reflections, T = 130 K), Z = 4, D_c = 1.68 g cm^{-3}, $F(000)$ = 1556, green blocks, crystal dimensions 0.125 × 0.20 × 0.425 mm, μ(Mo-Kα) = 1.81 mm^{-1}.

Data collection and processing. Details as for complex **1** except as follows: T = 130 K, ω scan speed 15° min^{-1}, 2θ range 0–50°; 5807 reflections measured, 5336 unique [R(merge) = 0.025], 3479 with $I > 2\sigma(I)$. Transmission factors 0.71–0.83.

Structure analysis and refinement. Direct methods. Full-matrix least-squares refinement with all non-hydrogen atoms anisotropic and hydrogens riding on bonded carbons, U_{iso} fixed at 0.03 Å^2; $w = [\sigma^2(F) + 0.0002F^2]^{-1}$. A partially occupied water site was assigned 0.5 occupancy. Refinement converged to R = 0.0483 and R' = 0.0430.

Crystal data for complex **3**. $C_{52}H_{40}Cl_4Cu_2N_{12}O_{16}$, M = 1357.8, monoclinic, space group $P2_1/c$, a = 12.332(2), b = 11.076(2), c = 39.78(2) Å, β = 90.06(2)°, U = 5434(3) Å^3 (by least-squares refinement on diffractometer angles for 24 centred reflections, T = 130 K), Z = 4, D_c = 1.66 g cm^{-3}, $F(000)$ = 2760, blue blocks, crystal dimensions 0.12 × 0.26 × 0.28 mm, μ(Mo-Kα) = 1.06 mm^{-1}.

Data collection and processing. Siemens P4/RA diffractometer, T = 130 K, θ–2θ scans with ω scan width ± 0.5° + Kα separation, θ scan speed 30° min^{-1}, Zr-filtered Mo-Kα radiation, 2θ range 0–45°, $+h$, $+k$, $\pm l$; 9776 reflections measured, 7146 unique [R(merge) = 0.024], 4950 with $I > 2\sigma(I)$. Absorption correction as for **1**, transmission factors 0.71–0.90.

Structure analysis and refinement. Direct methods. Full-matrix least-squares refinement with all non-hydrogen atoms anisotropic and hydrogens riding on bonded carbons, U_{iso} fixed at 0.024 Å^2; $w = [\sigma^2(F) + 0.0005F^2]^{-1}$. Refinement converged to R = 0.0516 and R' = 0.0501.

Additional material available from the Cambridge Crystallographic Data Centre comprises H-atom coordinates, thermal parameters and remaining bond lengths and angles.

Magnetic Measurements.—Samples were used as powders for magnetic susceptibility measurements. Magnetic susceptibilities were obtained between 5 and 300 K using a SHE 906 SQUID magnetometer, at a field strength of 1 kOe (10^3 A m^{-1}). Pascal's constants were used to estimate the correction for diamagnetism of the sample, and the temperature-independent paramagnetism contribution for each copper atom was taken as 60×10^{-6} emu mol^{-1}. A non-linear fitting program was used for the data analysis; the function minimized was $\Sigma(\chi_{obs} - \chi_{calc})^2/\chi_{obs}^2$.

Acknowledgements

This research was supported in part by the Fondo Nacional de Ciencia y Tecnologia, and by Fundacion Andes.

References

1 G. De Munno and G. Denti, *Inorg. Chim. Acta*, 1983, **74**, 199.
2 M. Ghedini, G. De Munno, G. Denti, A. M. Manotti Lanfredi and A. Tiripicchio, *Inorg. Chim. Acta*, 1982, **57**, 87.
3 L. K. Thompson, V. T. Chacko, J. A. Elvidge, A. B. P. Lever and R. V. Parish, *Can. J. Chem.*, 1969, **47**, 4141.
4 J. C. Dewan and L. K. Thompson, *Can. J. Chem.*, 1982, **60**, 121.
5 G. Maringui and E. C. Lingafelter, *Acta Crystallogr., Sect. B*, 1982, **38**, 620.
6 L. K. Thompson, *Can. J. Chem.*, 1983, **61**, 579.
7 L. K. Thompson, F. W. Hartstock, P. Robichaud and A. W. Hanson, *Can. J. Chem.*, 1984, **62**, 2755.
8 L. K. Thompson, A. V. Hanson and B. S. Ramaswamy, *Inorg. Chem.*, 1984, **23**, 2459.
9 G. Bullock, F. W. Hartstock and L. K. Thompson, *Can. J. Chem.*, 1983, **61**, 57.
10 L. K. Thompson, T. C. Woon, D. B. Murphy, E. J. Gabe, F. L. Lee and Y. Le Page, *Inorg. Chem.*, 1985, **24**, 4719.
11 T. C. Woon, R. McDonald, S. K. Mandal, L. K. Thompson, S. P. Connors and A. W. Addison, *J. Chem. Soc., Dalton Trans.*, 1986, 2381.
12 S. K. Mandal, L. K. Thompson, M. J. Newlands, F. L. Lee, Y. Le Page, J. P. Charland and E. J. Gabe, *Inorg. Chim. Acta*, 1986, **122**, 199.
13 L. K. Thompson, S. K. Mandal, E. J. Gabe, F. L. Lee and A. W. Addison, *Inorg. Chem.*, 1987, **26**, 657.
14 L. K. Thompson, S. K. Mandal, E. J. Gabe and J. P. Charland, *J. Chem. Soc., Chem. Commun.*, 1986, 1537.
15 L. K. Thompson, S. K. Mandal, J. P. Charland and E. J. Gabe, *Can. J. Chem.*, 1988, **66**, 348.
16 L. K. Thompson, F. L. Lee and E. J. Gabe, *Inorg. Chem.*, 1988, **27**, 39.
17 S. K. Mandal, L. K. Thompson, E. J. Gabe, J. P. Charland and F. L. Lee, *Inorg. Chem.*, 1988, **27**, 855.
18 B. Bleaney and K. D. Bowers, *Proc. R. Soc. London, Ser. A*, 1952, **214**, 451.
19 E. Leetle and L. Marion, *Can. J. Chem.*, 1952, **30**, 563.
20 G. M. Sheldrick, SHELXTL PLUS, User's Manual, Nicolet Instrument Co., Madison, WI, 1986.
21 *International Tables for X-Ray Crystallography*, Reidel, Boston, 1992, vol. C.
22 H. Hope and B. Moezzi, Program XABS, Chemistry Department, University of California, Davis.

Received 22nd July 1992; *Paper* 2/03911G